PERGAMON

Control Engineering Practice 9 (2001) 107–116

CONTROL ENGINEERING PRACTICE

www.elsevier.com/locate/conengprac

Nonlinear receding horizon sub-optimal guidance law for the minimum interception time problem

Mazen Alamir*

Laboratoire d'Automatique de Grenoble, UMR 5528, CNRS-INPG-UJF, BP 46 Domaine Universitaire, Saint Martin d'Hères, France

Received 8 September 1999; accepted 18 November 1999

Abstract

In this paper, a state feedback law that yields a sub-optimal solution of the minimum interception time problem is proposed. Sub-optimality is defined over the potential interception times that correspond to the system-compatible parabolic trajectories. Such trajectories are computed at each sampling instant and the whole procedure is reiterated in a receding horizon manner yielding a piece-wise continuous dynamic state feedback law. Simulations were proposed and the robustness was tested against the modelling errors. © *2001 Elsevier Science Ltd. All rights reserved.*

Keywords: Interception; Missile guidance; Nonlinear constrained control; Receding horizon; Real-time implementation

1. Introduction

In this paper, a feedback guidance law that leads to a sub-optimal solution of the minimum interception time problem is proposed. The difficulty in solving this problem stems from the fact that it corresponds to a nonlinear two-point boundary-value problem (TPBVP) that is hard to solve in real-time onboard configurations.

Several solutions have been proposed to derive simpler formulations of this optimal control problem. In Cheng and Gupta (1985) and Menon and Briggs (1990), singular perturbation technique is used to decouple the corresponding equations using arguments based on time scaling.

Another way to derive sub-optimal solutions for the above problem is to use a database of linear quadratic solutions defined around trajectories that have been memorized beforehand (Imado & Kuroda, 1990, 1992). Despite the large memory requirement needed for such an approach, the exhaustiveness of such a database is difficult to ensure.

Solutions based on coordinates transformation and linearization have been proposed. In Rusnak (1996), the optimal guidance law is developed in polar coordinates through the decomposition of the underlying optimal-control problem into two decoupled-optimal-control problems. A closed-form control solution is available in the radial direction and a time-varying linear dynamic system is solved for control in the transverse direction.

More recently, Dougherty and Speyer (1997) proposed an iterative algorithm that gives a sub-optimal solution to the TPBVPs ordinary differential equations that result from the maximum principle. The influence of the uncertainty on the aerodynamic coefficients is then studied.

In Song and Tahk (1998) and in the preceding work, they proposed an approach that identifies the optimal feedback using neural-network approximations. In these works, the nonlinear function solution of the optimal-control problem (here maximal terminal-velocity under interception constraint) are identified based on the off-line solution of the same problem for several scenarios using initial conditions for both the target and the missile. While conceptually attractive, this solution may present some drawbacks when applied outside the space domain used in the neural-network learning.

The starting point of the approach proposed in this paper lies in the following question:

"Is it clear that an approximated solution of the exact equations representing the necessary conditions for optimality is better than an exact solution of some a priori sub-optimal requirement?".

* Fax: + 04-76-82-63-88.

E-mail address: mazen.alamir@inpg.fr (M. Alamir).

PII: S0967-0661(00)00085-X

The legitimacy of the above question increases when one takes into consideration the unavoidable uncertainties about the values of the aerodynamic coefficients as well as the future motion of the target.

Based on the idea above, this paper proposes a simple and intuitive way to define a sub-optimal problem of the exact minimum-interception time problem that is easy to solve. The solution of the sub-optimal problem is then used in a receding horizon manner to yield a feedback law.

More precisely, sub-optimality is achieved from the fact that one searches for the minimum interception time in the scalar space of interception times that are defined over system-compatible parabolic trajectories. System-compatible parabolic trajectories are parabolic trajectories in the (x, h) plane that pass through the actual position of the missile and the target's position at the interception instant. They have an initial slope that is compatible with the initial missile's path angle γ (see Fig. 1 hereafter). Furthermore, compatibility also includes the feasibility under the control's saturation constraints.

The reason why such a sub-optimal interception time (and trajectory) is easy to find is that the underlying equation to be solved is a scalar algebraic one. The computation of the solution of this resulting equation is done at the beginning of each sampling period. However, during the sampling period, the feedback law is defined in order to track the corresponding parabolic interception trajectory.

In this paper, two procedures are proposed to solve the underlying scalar nonlinear sub-optimality equation, yielding two different feedback laws. The real-time implementability of the resulting feedback laws is investigated together with their robustness against the modelling error of the aerodynamic coefficients.

The paper is organized as follows:

The missile's dynamic equations are described in Section 2. Section 3 states the problem under consideration. The derivation of the feedback law is presented in Section 3 while in Section 4, numerical simulations are proposed to illustrate the efficiency of the proposed laws as well as their robustness against the modelling errors.

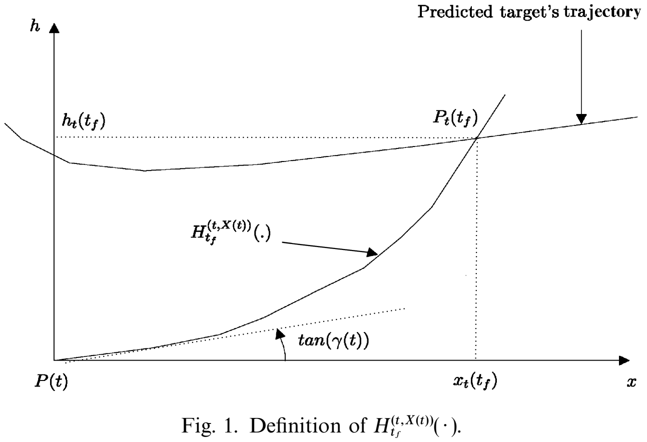

Fig. 1. Definition of $H_{t_f}^{(t,X(t))}(\cdot)$.

Table 1
Aerodynamic coefficients values vs. Mach number

M	C_{L_α}	C_{D_0}	k
0.2	9.31	0.242	0.110
0.8	7.65	0.211	0.135
0.93	7.73	0.255	0.134
1.05	9.74	0.406	0.108
1.3	10.03	0.444	0.108
1.6	9.28	0.370	0.116
2.4	9.02	0.254	0.120
3.5	8.02	0.190	0.134
5.0	7.16	0.149	0.153

2. The Missile's dynamic equations

Consider the classical equations of motion in the vertical plane (x, h). The state of the missile is defined by its four components: the velocity v, the flight path angle γ and the position coordinates (x, h):

$$\dot{v} = (T\cos\alpha - D)/m - g\sin\alpha, \tag{1}$$

$$\dot{\gamma} = (L + T\sin\alpha)/(mv) - \frac{g}{v}\cos\gamma, \tag{2}$$

$$\dot{x} = v\cos\gamma, \quad \dot{h} = v\sin\gamma, \tag{3,4}$$

where the aerodynamic moment L and drag force D are given by

$$L = \tfrac{1}{2}\rho v^2 S C_L, \quad C_L = C_{L_\alpha}(\alpha - \alpha_0), \tag{5a}$$

$$D = \tfrac{1}{2}\rho v^2 S C_D, \quad C_D = C_{D_0} + kC_L^2. \tag{5b}$$

The experimental values of the parameters C_{L_α}, C_{D_0} and k are given in Table 1 as a function of the Mach number $M = M(v, h)$. Note also that the air density ρ is a function of the altitude h, that is $\rho(h) = \rho_0\exp(-\kappa h/h_0)$.

Finally, the missile mass and thrust are a priori given functions of the time t (see Fig. 4). The angle of attack α is used as the control variable which should satisfy the following inequality constraint

$$\alpha_{min} \leqslant \alpha \leqslant \alpha_{max}. \tag{6}$$

In what follows, the following compact notations are used

$$X := (v, \gamma, x, h)^{\mathrm{T}}, \quad P := (x, h). \tag{7}$$

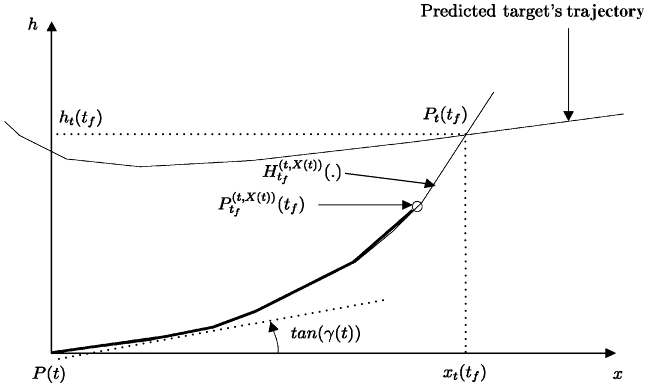

Fig. 2. t_f is to be chosen such that $P_t(t_f) = P_{t_f}^{(t,X(t))}(t_f)$.

3. Problem statement

It is assumed that the target's movement is computed by a ground system and transmitted to the missile during the mid-course guidance phase. The accuracy of this information is not explicitly discussed in this paper. The possible error in predicting the target's movement is to be naturally "*absorbed*" by the robustness margin of the new feedback law.

Therefore, it is assumed that at each instant t (including instants t that belong to the near future), the position of the target is given by some known functions of time

$$P_t(t) := \begin{pmatrix} x_t(t) \\ h_t(t) \end{pmatrix}$$

(the subscript t in the above notation is used to denote "*target*"-related functions).

The aim of this work is to propose a simple and real-time implementable state feedback law

$$\alpha = \alpha(t, X)$$

that corresponds to some sub-optimal solution of the problem of minimum interception time. Indeed, the computation of the exact feedback optimal solution of the constrained free final time optimal-control problem above may not be suitable for real-time implementation requirements. The key point is then to exploit particular features to derive a simple "*heuristic*" feedback algorithm.

4. Derivation of the feedback law

4.1. Basic idea

The key point to note is that the flight path angle γ is "*easily*" controlled by α. This is true at the beginning because of the higher values of the thrust T enabling γ to be controlled using the term $T\sin\alpha$. When the thrust stops, it is the aerodynamic term $L = \frac{1}{2}\rho v^2 SC_L$ that becomes high enough (because of v^2) to control γ. Simple computation of the relative importance of the different terms of (2) during the different phases enables the above statements to be strengthened. (Examination of the proposed simulations at the end of this paper is another way to check them.) This is especially true when system-compatible trajectories are to be tracked.

Based on the above fact and taking into account that constraint (6) yields small admissible values for α. Eq. (2) enables one to define the following feedback law for each reference profile on γ, say $\gamma_{ref}(t)$:

$$\alpha(\gamma_{ref}(\cdot), X, t) =$$

$$Sat_{\alpha_{min}}^{\alpha_{max}} \left\{ \frac{\frac{1}{2}\rho v^2 SC_{L_\alpha}\alpha_0 + mv[\dot{\gamma}_{ref} - \mu(\gamma - \gamma_{ref})] + mg\cos}{T + \frac{1}{2}\rho v^2 SC_{L_\alpha}} \right\}, \tag{8}$$

where $Sat_{\alpha_{min}}^{\alpha_{max}}\{\cdot\}$ is the saturation function given by

$$Sat_{\alpha_{min}}^{\alpha_{max}}\{\alpha\} := \begin{cases} \alpha_{min} & \text{if } \alpha \leqslant \alpha_{min}, \\ \alpha_{max} & \text{if } \alpha \geqslant \alpha_{max}, \\ \alpha & \text{otherwise.} \end{cases} \tag{9}$$

Note that (8) depends explicitly on t because of the varying quantities $m(t)$ and $T(t)$. Note also that in the absence of saturation, and under the approximation $\sin(\alpha) \approx \alpha$, the feedback law (8) forces the tracking error $e(t) = \gamma(t) - \gamma_{ref}(t)$ to satisfy

$$\dot{e}(t) = -\mu e(t), \quad \mu > 0.$$

Therefore, at each instant t, a suitable state-dependent reference trajectory

$$\gamma_{ref}^{(t,X(t))}(X(\cdot)) \tag{10}$$

is computed (see Section 4.2) based on the present state $X(t)$ of the missile and the predicted movement of the target. Now, injecting (10) into (8) yields the time-varying feedback law

$$\alpha(\gamma_{ref}^{(t,X(t))}(X(\cdot)), X(\cdot), \cdot). \tag{11}$$

The whole procedure is then implemented in a receding horizon manner (Keerthi & Gilbert, 1988; Mayne & Michalska, 1990; Michalska & Mayne, 1991; Alamir & Bornard, 1994). More precisely, a sampling period $T > 0$ is first defined (T is often omitted in order to simplify the expressions. Namely, k is used to designate kT while $X(k)$ stands for $X(kT)$). Then the following receding horizon piece-wise continuous state feedback is applied over the time interval $[kT, (k+1)T]$:

$$\alpha(\gamma_{ref}^{(k,X(k))}(X(\cdot)), X(\cdot), \cdot), \quad \text{over } [kT, (k+1)T]. \tag{12}$$

Note that in (12), the function $\gamma_{ref}^{(k,X(k))}(\cdot)$ is computed at $(kT, X(kT))$ and the same state-dependent relation $\gamma_{ref}^{(k,X(k))}(X)$ is maintained over the time interval $[kT, (k+1)T]$. This is done for real-time implementation requirements since the computation of the function $\gamma_{ref}^{(k,X(k))}(\cdot)$ may be relatively heavy (in comparison with some given analytical expressions).

At instant $(k+1)T$, a new function

$$\gamma_{ref}^{(k+1,X(k+1))}(X(\cdot))$$

is computed and the whole procedure is repeated. Section 4.2 is dedicated to explain how the reference trajectory $\gamma_{ref}^{(t,X(t))}(\cdot)$ is generated in order to meet the sub-optimal time-interception requirement.

4.2. *Definition of* $\gamma_{ref}^{(t,X(t))}(\cdot)$

- Let t and $X(t)$ be given. These are fixed throughout the following sequel.
- For all $t_f > t$, let $P_t(t_f)$ be the predicted position of the moving target and let $H_{t_f}^{(t,X(t))}(x)$ be the unique parabola that satisfies the following conditions (see Fig. 1):

$$H_{t_f}^{(t,X(t))}(x(t)) = h(t), \tag{13a}$$

$$H_{t_f}^{(t,X(t))}(x_t(t_f)) = h_t(t_f), \tag{13b}$$

$$\frac{\mathrm{d}H_{t_f}^{(t,X(t))}}{\mathrm{d}x}(x(t)) = \tan(\gamma(t)), \tag{13c}$$

in other words, $H_{t_f}^{(t,X(t))}(x)$ is the unique parabola in the plane (x, h) that passes through the points $P(t)$ and $P_t(t_f)$ and has the slope $\tan(\gamma(t))$ at $P(t)$. This can be written as follows:

$$H_{t_f}^{(t,X(t))}(x) := a_2^{(t,X(t))}(t_f)x^2 + a_1^{(t,X(t))}(t_f)x + a_0^{(t,X(t))}(t_f), \tag{14}$$

where the expressions of the $a_i^{(t,X(t))}(t_f)$ are given by Eqs. (A.1a)–(A.1c) (see Appendix A).
- The state-dependent reference trajectory $\gamma_{ref}^{(t,X(t))}(X)$ to be defined will be of the following form:

$$\gamma_{ref}^{(t,X(t))}(\cdot) := A\tan\left(\frac{\mathrm{d}H_{t_f}^{(t,X(t))}}{\mathrm{d}x}(\cdot)\right) \tag{15}$$

for some convenient choice of the final time t_f. The remainder of this section explains this choice of t_f.
- Note that the parabola above represents a reference trajectory in the plane (x, h) that is compatible with the initial conditions $(t, X(t))$ of the missile. However, it is not an interception trajectory for an arbitrary choice of t_f.
- To understand this, let $X_{t_f}^{(t,X(t))}(\tau)$ denote the solution of (1)–(4) for $\tau > t$ that starts at $(t, X(t))$ and under feedback (8) in which γ_{ref} and $\dot{\gamma}_{ref}$ are taken as follows:

$$\begin{aligned}\gamma_{ref} &:= A\tan(\mathrm{d}H_{t_f}^{(t,X(t))}/\mathrm{d}x(\cdot)) \\ &= A\tan(2a_2^{(t,X(t))}(t_f)x + a_1^{(t,X(t))}(t_f)),\end{aligned} \tag{16a}$$

$$\begin{aligned}\dot{\gamma}_{ref} &:= \frac{1}{1 + (\mathrm{d}H_{t_f}^{(t,X(t))}/\mathrm{d}x)^2}\frac{\mathrm{d}^2H_{t_f}^{(t,X(t))}}{\mathrm{d}x^2}\dot{x} \\ &= \frac{2a_2^{(t,X(t))}(t_f)v\cos(\gamma)}{1 + (2a_2^{(t,X(t))}(t_f)x + a_1^{(t,X(t))}(t_f))^2}\end{aligned} \tag{16b}$$

in other words, let $X_{t_f}^{(t,X(t))}(\tau)$ be the closed-loop trajectory when the feedback is designed to follow the parabola $H_{t_f}^{(t,X(t))}$ in the plane (x, h). (Note that this may be done without violating the constraints on the control α since the trajectory is chosen to be compatible with the missile's configuration at $(t, X(t))$.)
- According to the above definition, one has (see Fig. 3)

$$h_{t_f}^{(t,X(t))}(\tau) = H_{t_f}^{(t,X(t))}(x_{t_f}^{(t,X(t))}(\tau)) \quad \forall \tau > t. \tag{17}$$

However, for arbitrarily chosen t_f there is no reason to have interception at t_f, that is (see Fig. 2)

$$P_t(t_f) \neq P_{t_f}^{(t,X(t))}(t_f) \quad \text{in general.} \tag{18}$$

- Owing to (17), in order for t_f to be an interception instant, it has to satisfy the following condition:

$$\begin{aligned}\beta^{(t,X(t))}(t_f) &:= \int_t^{t_f} v_{t_f}^{(t,X(t))}(\tau)\,\mathrm{d}\tau \\ &\quad - \int_{x(t)}^{x_t(t_f)}\left[1 + \left(\frac{\mathrm{d}H_{t_f}^{(t,X(t))}}{\mathrm{d}x}\right)^2\right]^{1/2}\mathrm{d}x = 0,\end{aligned} \tag{19}$$

note that (19) states that the length of the curve defined by (17) between $\tau = t$ and t_f is equal to the length of the portion of parabola delimited by the points $P(t)$ and $P_t(t_f)$ which with (17) clearly implies that interception occurs at t_f.

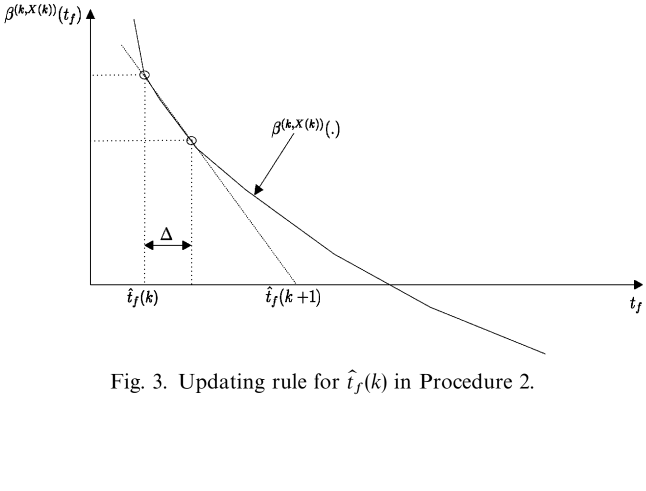

Fig. 3. Updating rule for $\hat{t}_f(k)$ in Procedure 2.

- Therefore, all it remains to do is to solve the equation

$$\beta^{(t,X(t))}(t_f) = 0 \tag{20}$$

in the *scalar unknown* t_f. Another way to underline the basic feature of the proposed approach is to say that the combination of (8) and (15) enables the open-loop interception problem (that is later used in a receding horizon scheme to yield a feedback law) to be parameterized by only one parameter, namely t_f. This readily simplifies the generation of the open-loop solution and hence gives the possibility of implementing it in a real-time closed-loop receding-horizon configuration.

To do this, the two following procedures are proposed.

4.2.1. Procedure P1

Compute $\beta^{(t,X(t))}(t_i)$ for an increasing sequence of future instants $t < t_1 < t_2 < \cdots$ until a sign inversion is obtained. The solution t_* can then be obtained by dichotomy until some admissible precision is reached. Note that each computation of $\beta(t_i, t, X(t))$ corresponds to the integration of the system equations (1)–(4).

According to the procedure P1, the computation of $\hat{t}_f(t, X(t))$, solution of (20) is performed by means of Algorithm 1.

Algorithm 1. The function $\hat{t}_f^{(1)}(t, X(t))$ for procedure $P1$

```
Algorithm $\hat{t}_f^{(1)}(t, X(t))$
1: **Fixed parameters**: $\Delta > 0$ (time step),
                         $\varepsilon > 0$ (final precision)
2: **Initialization**   $\beta \leftarrow \beta^{(t,X(t))}(t)$;   $t^+ = t$
3: **Repeat**
     (1) $t^+ \leftarrow t^+ + \Delta$;   $\beta^+ \leftarrow \beta^{(t,X(t))}(t^+)$
     (2) **If** $\beta \cdot \beta^+ > 0$ **then** $\beta \leftarrow \beta^+$ **end if**
4: **Until** $\beta \cdot \beta^+ < 0$
5: $t_1 \leftarrow t^+ - \Delta$;   $t_2 \leftarrow t^+$;   $\beta_1 \leftarrow \beta$;   $\beta_2 \leftarrow \beta^+$
6: **Do while** $(t_2 - t_1) > \varepsilon$
     (1) $t_c \leftarrow (t_1 + t_2)/2$;   $\beta_c \leftarrow \beta^{(t,X(t))}(t_c)$
     (2) **If**   $\beta_1 \cdot \beta_c > 0$ **then** $t_1 \leftarrow t_c$ **Else** $t_2 \leftarrow t_c$ **end if**
7: **end do while**
8: $\hat{t}_f(t, X(t)) \leftarrow t_c$
```

4.2.2. Procedure P2

The authors believe that the procedure $P1$ may be convenient even in the presence of fast real-time computation requirements. Nevertheless, hereafter, an approximated version is proposed based on the simple gradient descent scheme in which the system Eqs. (1)–(4) are to be integrated only two times at each sampling period (see Fig. 4).

The principle is still to solve the equation $\beta^{(t,X(t))}(t_f) = 0$ defined above. However, the "*distributed*" Newton method is used instead of dichotomy. In the "*distributed*" Newton method, the Newton method iterations are distributed over the successive sampling periods. One step is performed at each sampling period.

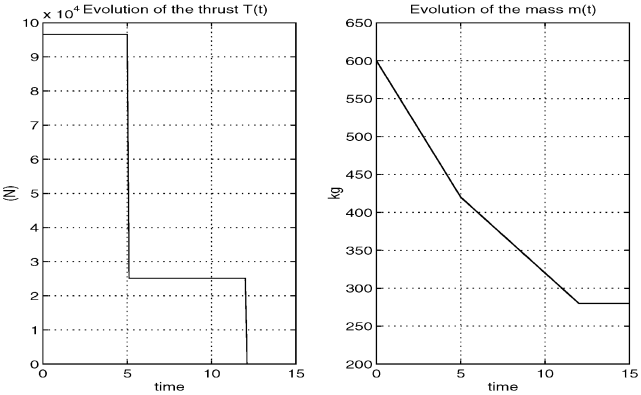

Fig. 4. Evolution of the mass $m(t)$ and the thrust $T(t)$.

More precisely, let $\hat{t}_f(k)$ be the adopted solution at instant kT. Consider the following updating rule:

$$\hat{t}_f(k+1) := \hat{t}_f(k) + Sat_{-\mathrm{d}t_{max}}^{+\mathrm{d}t_{max}} \left\{ \frac{-\Delta}{\beta^{(k,X(k))}(\hat{t}_f(k) + \Delta) - \beta^{(k,X(k))}(\hat{t}_f(k))} \right\}, \tag{21}$$

where $\Delta > 0$ is small time step and $\mathrm{d}t_{max}$ is some maximal admissible updating difference used to avoid related numerical singularity problems. Note that in the case of procedure 2, one gets a dynamic state feedback in which $\hat{t}_f(k)$ represents an internal state of the controller.

The use of the distributed Newton descent implicitly suggests that function $\beta^{(k,X(k))}(\cdot)$ is convex, over the time interval of interest at least. It is obviously hard to prove this intuition in the general case. However, one can easily admit that for a rather simple target movements, this might be often true.

4.3. Summary of the feedback design

The above sequel can be summed up as follows.

4.4. Feedback 1

From (8), (16) and Algorithm 1 the feedback law is defined for all $\tau \in [0, T[$ by

$$\alpha(kT + \tau, X, k, X(k)) = Sat_{\alpha_{min}}^{\alpha_{max}} \left\{ \frac{\frac{1}{2}\rho v^2 S C_{L_\alpha} \alpha_0 + mv[\dot{\gamma}_{ref} - \mu(\gamma - \gamma_{ref})] + mg\cos(\gamma_{ref})}{T + \frac{1}{2}\rho v^2 S C_{L_\alpha}} \right\}, \tag{22a}$$

$$\gamma_{ref}(X, k, X(k)) := A\tan(2a_2^{(k,X(k))}(\hat{t}_f^{(1)}(k, X(k)))x + a_1^{(k,X(k))}(\hat{t}_f^{(1)}(k, X(k)))), \tag{22b}$$

$$\dot{\gamma}_{ref}(X,k,X(k)):= \frac{2a_2^{(k,X(k))}(\hat{t}_f^{(1)}(k,X(k)))v\cos(\gamma)}{1+(2a_2^{(k,X(k))}(\hat{t}_f^{(1)}(k,X(k)))x+a_1^{(k,X(k))}(\hat{t}_f^{(1)}(k,X(k))))^2}, \tag{22c}$$

$$\hat{t}_f^{(1)}(k,X(k)) \quad \text{Computed by Algorithm 1.} \tag{22d}$$

4.5. *Feedback 2*

The first three equations remain unchanged, the computation of $\hat{t}_f$ however is performed by means of the controller internal state $\hat{t}_f(k)$, namely, for all $\tau \in [0, T[$

$$\alpha(kT+\tau, X, k, X(k)) = Sat_{\alpha_{min}}^{\alpha_{max}}\left\{\frac{\frac{1}{2}\rho v^2 SC_{L_\alpha}\alpha_0 + mv[\dot{\gamma}_{ref} - \mu(\gamma-\gamma_{ref})] + mg\cos(\gamma_{ref})}{T+\frac{1}{2}\rho v^2 SC_{L_\alpha}}\right\}, \tag{23a}$$

$$\gamma_{ref}(X,k,X(k)):= A\tan(2a_2^{(k,X(k))}(\hat{t}_f(k))x + a_1^{(k,X(k))}(\hat{t}_f(k))), \tag{23b}$$

$$\dot{\gamma}_{ref}(X,k,X(k)):= \frac{2a_2^{(k,X(k))}(\hat{t}_f(k))v\cos(\gamma)}{1+(2a_2^{(k,X(k))}(\hat{t}_f(k))x+a_1^{(k,X(k))}(\hat{t}_f(k)))^2}, \tag{23c}$$

$$\hat{t}_f(k+1):= \hat{t}_f(k) + Sat_{-\mathrm{d}t_{max}}^{+\mathrm{d}t_{max}}\left\{\frac{-\Delta}{\beta^{(k,X(k))}(\hat{t}_f(k)+\Delta) - \beta^{(k,X(k))}(\hat{t}_f(k))}\right\}. \tag{23d}$$

5. Simulation results

5.1. *Model's parameters*

The experimental values for the aerodynamic coefficients are given in Table 1. The evolution of the mass and the thrust are depicted in Fig. 2. Furthermore, the following values are used: $S = 0.25$, $\alpha_{\min} = -\alpha_{\max} = -20°$.

5.2. *The target's movement*

The two following movements for the target are used:

$$x_t(t) = 450t, \quad h_t(t) = 7000 \tag{24}$$

and

$$x_t(t) = 450t, \quad h_t(t) = 7000 + 3t^2. \tag{25}$$

5.3. *Initial conditions*

Consider the following initial state for the missile:

$$x(0) = 0, \quad h(0) = 3000, \quad \gamma(0) = -40°, \quad v(0) = 100 \text{ m/s}, \tag{26}$$

note that the initial values $\gamma(0) = -40°$ are quite penalizing when considering the target's trajectory.

5.4. *Results using Feedback 1*

5.4.1. *Simulation parameters*

- $\mu = 10$ (see (22a)).
- Integration time step $\mathrm{d}t = 0.05$ for predictive integration used to compute $X_{t_f}^{(t,X(t))}$ (and hence $\beta^{(k,X(k))}$).
- Time step $\Delta = 0.5$ s and $\varepsilon = 0.01$ in Algorithm 1.
- Sampling period $T = 0.2$ s.

5.4.2. *Results*

In this first set of simulations, the feedback law (22) is used. Simulation results for target's movement (24) are presented in Fig. 5. In this figure, the following features can be observed:

- the evolution of x-coordinates for target and missile;
- the evolution of h-coordinates for target and missile;
- the evolution of the coordinate differences $x_t(t) - x(t)$ and $h_t(t) - h(t)$. It is in this figure that interception may be localized in time;

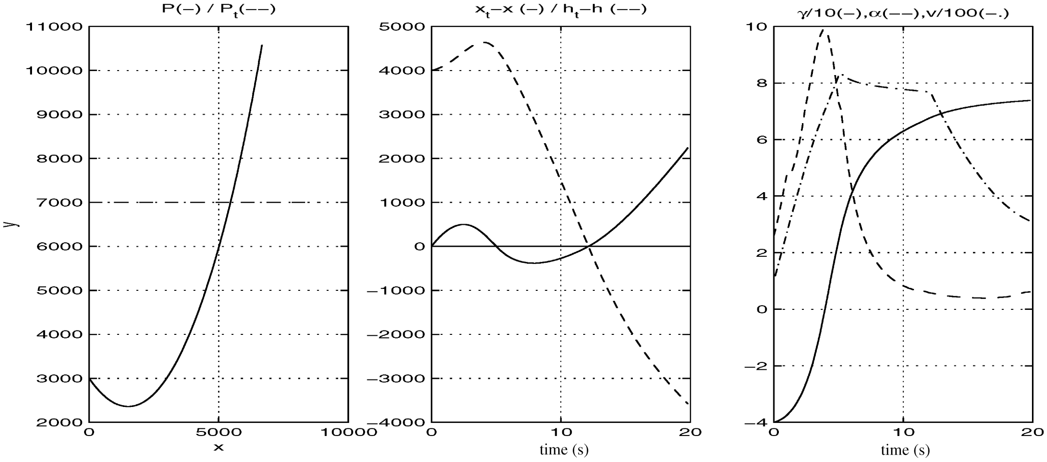

Fig. 5. Simulation results for target's movement (24) and with exact model and Feedback 1.

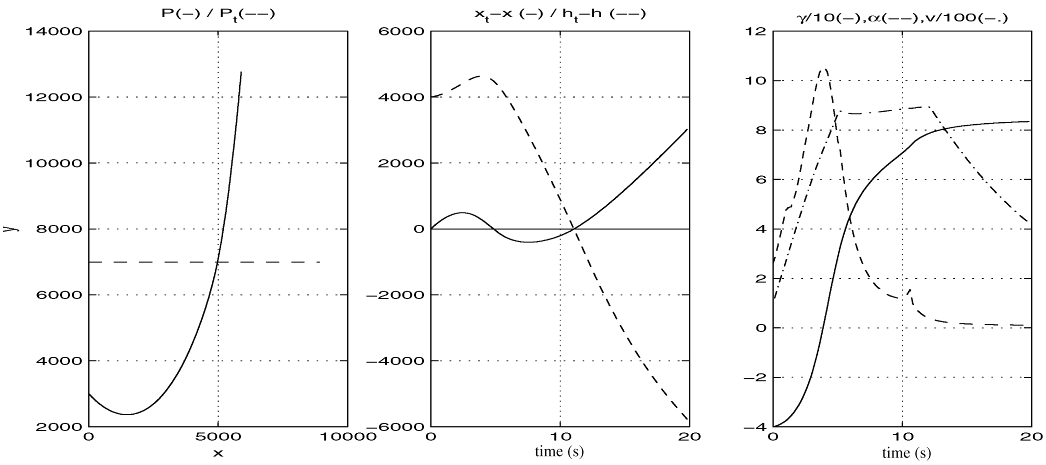

Fig. 6. Simulation results for target's movement (24) with modelling error and Feedback 1.

- the evolution of path angle $\gamma(t)$;
- the evolution of the control action $\alpha(t)$;
- the evolution of the missile's velocity $v(t)$.

The same results are given in Fig. 6 for the same target's motion (24) when the controller uses an erroneous model. This last one differs from the "*true*" one by the values of the aerodynamic coefficients. More precisely, the controller uses the following values:

$$C'_{D_0} := \lambda_1 C_{D_0}, \quad k' = \lambda_2 k, \quad C'_{L_\alpha} = \lambda_3 C_{L_\alpha}, \tag{27}$$

where

$$\lambda_1 = 0.8, \quad \lambda_2 = 0.6, \quad \lambda_3 = 1.25, \tag{28}$$

namely, a relative error of -20, -40 and 25% are assumed on C_{D_0}, k and C_{L_α}, respectively.

The simulations depicted in Fig. 6 show the robustness of the proposed feedback law and underline the benefit of the receding horizon implementation. This can be more clearly understood in Fig. 7. In this figure, the evolution of the predicted interception times $\hat{t}^{(1)}(k, X(k))$ at the successive sampling instants are compared when an exact or erroneous model is supplied to the controller. Recall that in the case of the exact model, $\hat{t}^{(1)}(k, X(k))$ is practically constant due to the use of *Procedure* 1. Indeed, in this case, the quasi exact solution of (20) that does not change in the absence of disturbances is obtained from the beginning. However, in the case where the model used by the controller is different from the effective one, $\hat{t}^{(1)}(k, X(k))$ are continuously updated since the controller predictions are different from the effective closed-loop trajectory.

Note that since $C'_{D_0} < C_{D_0}$, the air resistance to the missile's acceleration is lower than in the nominal case. This explains why the interception time is reduced in the presence of the modelling errors considered for this example, and strengthens the quasi-optimal nature of the proposed law in the sense of interception time.

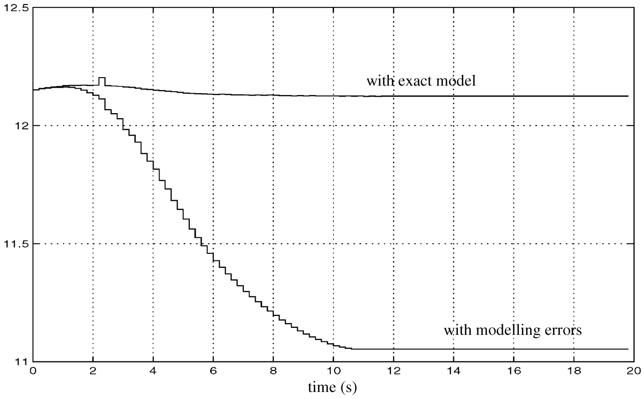

Fig. 7. Evolution of predicted interception times $\hat{t}^{(1)}(k, X(k))$ (in seconds) for target's movement (24) and Feedback 1.

Figs. 8–10 present the same results as in Figs. 5–7 but under the following conditions:

- the target's trajectory (25) is used;
- the following coefficient are used in (27) to define the modelling errors:

$$\lambda_1 = 1.2, \quad \lambda_2 = 0.6, \quad \lambda_3 = 1.25. \tag{29}$$

Note that in this case, the interception time is higher than in the nominal case since with $\lambda_1 = 1.2$, the air resistance to the missile acceleration is higher. Again, the proposed feedback shows good robust behavior that is necessary to compensate for the drawback of the extrapolating nature of the target's trajectory. Indeed, the predicted target's trajectory is to be continuously updated by the ground system. The above simulations enables one to predict a good adaptation of the proposed state feedback that may compensate for the effects of the extrapolation errors.

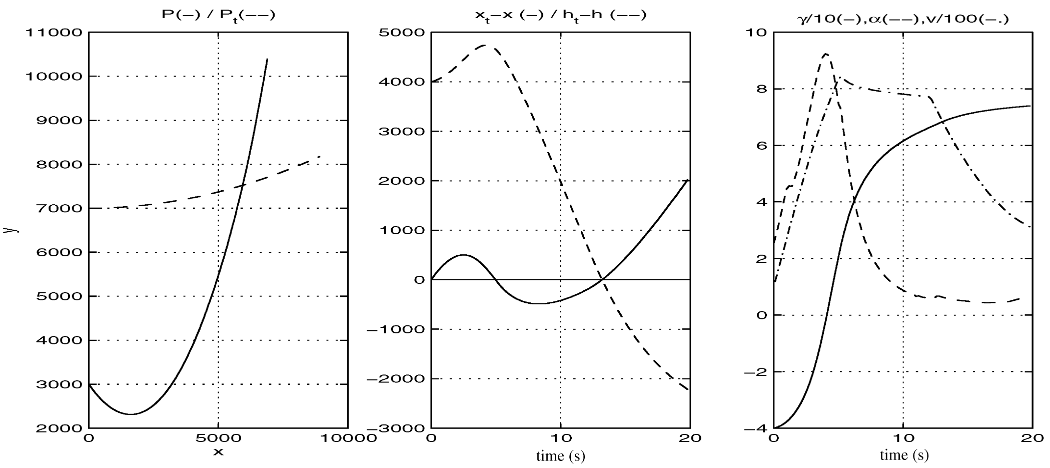

Fig. 8. Simulation results for target's movement (25) and with exact model and Feedback 1.

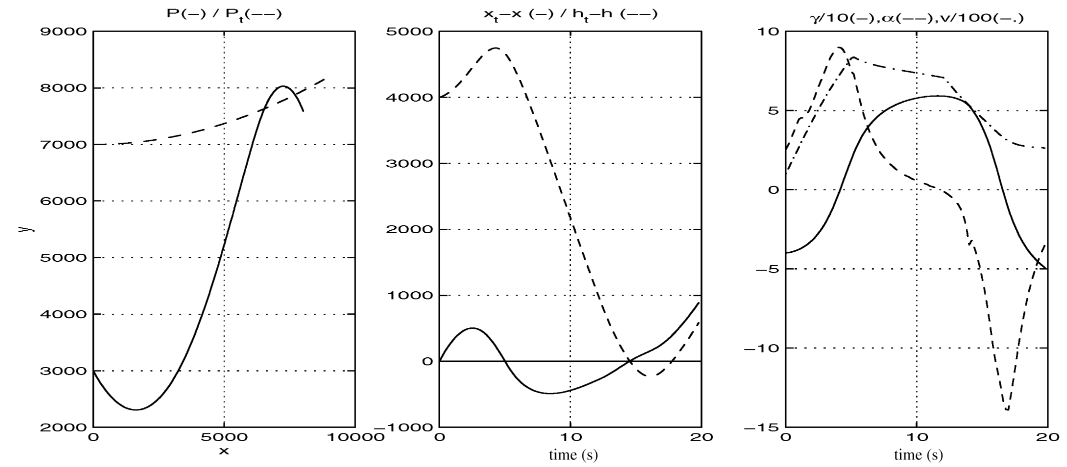

Fig. 9. Simulation results for target's movement (25) with modelling error and Feedback 1.

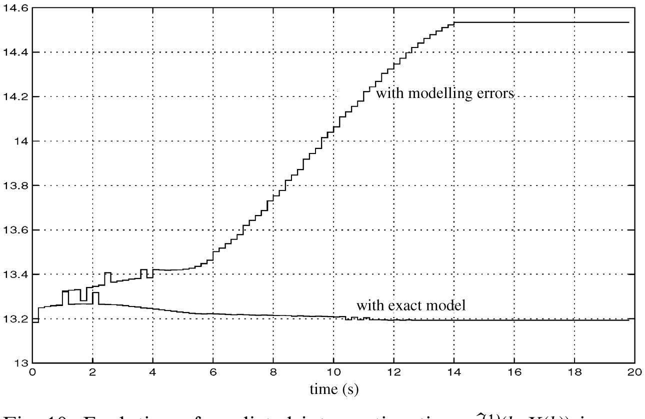

Fig. 10. Evolution of predicted interception times $\hat{t}^{(1)}(k, X(k))$ in seconds for target's movement (25) and Feedback 1.

5.5. Results using Feedback 2

In this section, the simulation of *Feedback* 2 are presented. To do this, the second scenario presented above is considered. Namely, the target's motion defined by (25). Again, two simulations are proposed. The first with the exact model used by the controller and the second with the erroneous model defined by (27) and (29).

The initial value $\hat{t}_f(0) = 3$ is considered while the parameter $\Delta = 0.1$ is used for the updating rule (23d). Finally, the maximal updating time step $\mathrm{d}t_{\max} = 10$ is adopted.

Figs. 11 and 12 show the closed-loop behavior for exact and erroneous models, respectively. Fig. 13 shows the evolution of the controller's internal state $\hat{t}_f(k)$ updated using (23d) according to the definition of Feedback 2. Note that the quite fast convergence of $\hat{t}_f(k)$ that enables one to state that the use of this dynamic search for the solution of (20) gives results that are very close to those given by the search for an "*exact*" solution at each sampling instant.

5.6. Computation times

In this section, computation times of Feedbacks 1 and 2 are compared in order to appreciate their real-time

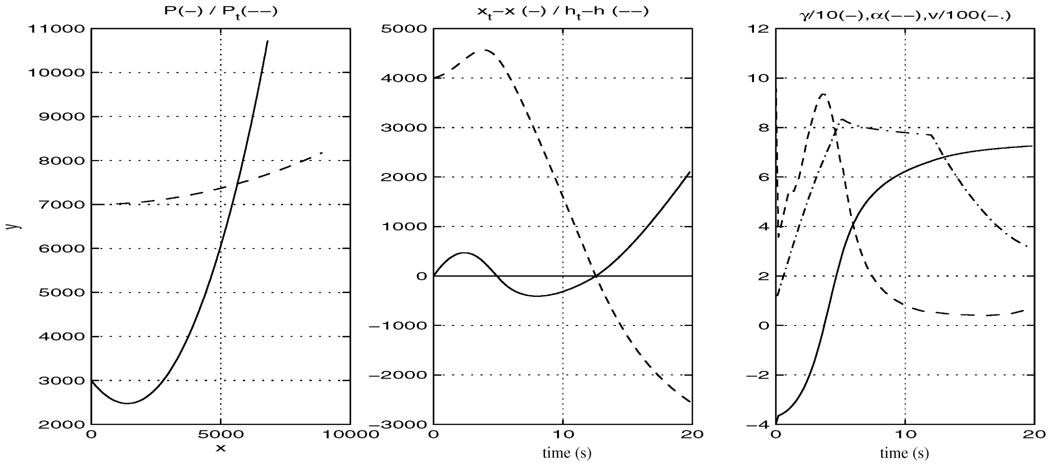

Fig. 11. Simulation results for target's movement (25) and with exact model and Feedback 2.

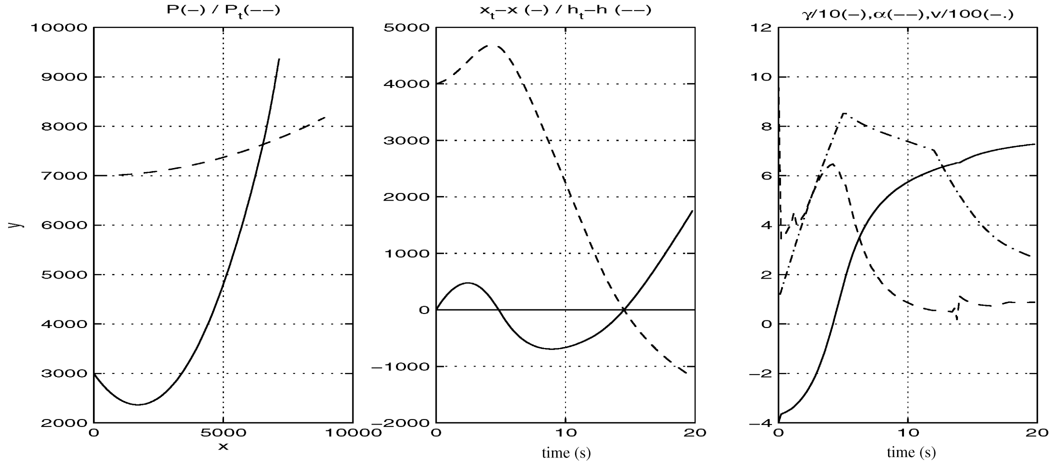

Fig. 12. Simulation results for target's movement (25) with modelling error and Feedback 2.

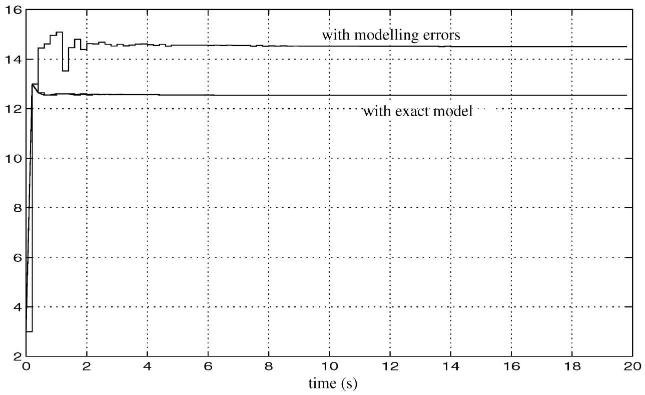

Fig. 13. Evolution of predicted interception times $\hat{t}_f(k)$ in seconds for target's movement (25) and Feedback 2.

implemention. It is clear that the computation time of the key tasks to be considered is the evaluation of $\hat{t}^{(1)}(k, X(k))$ in Feedback 1 and that of $\hat{t}_f(k)$ in Feedback 2.

The computation times have been estimated using the following procedure. For Feedback 1, the first scenario in which the maximum computation time for $\hat{t}^{(1)}(k, X(k))$, $k = 1, \dots$ is reported is considered. This is because the number of computations needed may vary slightly with k. Note that $\Delta = 0.5$ and $\varepsilon = 0.01$ are considered. Since the computations of the updating rule (23d) are always the same for Feedback 2, and since a single update is too fast, the computation time is calculated by invoking the updating rule 100 times.

Computations were performed on a PC Pentium III, 450 MHz. The results are shown in Table 2.

Recall that the computation times above are to be compared with the sampling period of 0.2 s. The implemention of Feedback 2 is clearly proved while that of Feedback 1 may strongly depend on the parameters used (Δ, ε and the sampling period), as well as on the on-board systems. Therefore, it must be checked in a more detailed manner. Recall, however, that in both feedbacks, the control used within the sampling

Table 2
Computation time (in s) for Feedbacks 1 and 2

Feedback 1	Feedback 2
0.04	0.0004

Appendix A

Expressions of the parabola coefficients $a_i^{(t,X(t))}(t_f)$

$$a_2^{(t,X(t))}(t_f) := \frac{h_t(t_f) - h(t) + (x(t) - x_t(t_f))\tan(\gamma(t))}{[x_t(t_f) - x(t)]^2}, \quad \text{(A.1a)}$$

$$a_1^{(t,X(t))}(t_f) := \frac{2x(t)[h(t) - h_t(t_f)] + [x_t^2(t_f) - x^2(t)]\tan(\gamma(t))}{[x_t(t_f) - x(t)]^2}, \quad \text{(A.1b)}$$

$$a_0^{(t,X(t))}(t_f) := \frac{[x_t^2(t_f) - 2x_t(t_f)x(t)]h(t) + x^2(t)h_t(t_f) + x_t(t_f)x(t)[x(t) - x_t(t_f)]\tan(\gamma(t))}{[x_t(t_f) - x(t)]^2}. \quad \text{(A.1c)}$$

period is still a feedback and therefore, the sampling period (equal to 0.2 s in the simulations) may be augmented.

6. Conclusion

In this paper, a new feedback law that yields a sub-optimal solution of the minimum interception time problem is proposed. The derivation of the proposed feedback law is based on intuitive geometric arguments and can therefore be easily understood by practitioners. The robustness of the proposed feedback law against aerodynamic coefficient modelling errors have been successfully tested. It is worth noting that the approach can easily be generalized to handle a combined criterion on interception time and final speed by using higher-order polynomials to define system-compatible trajectories. This leads to a two-dimensional algebraic equation to be solved. However, real-time implemention is still to be adequately rechecked.

Acknowledgements

The author would like to thank the anonymous reviewers for their valuable remarks.

References

Alamir, M., & Bornard, G. (1994). On the stability of receding horizon control of nonlinear discrete-time systems. *Systems and Control Letters*, *23*, 291–296.

Cheng, V. H. L., & Gupta, N. K. (1985). Advanced midcourse guidance for air-to-air missiles. *Journal of Guidance, Control and Dynamics*, *9*(2), 135–142.

Dougherty, J. J., & Speyer, J. L. (1997). Near optimal guidance law for ballistic missile interception. *Journal of Guidance, Control and Dynamics*, *20*(2), 355–361.

Imado, F., & Kuroda, T. (1990). Optimal midcourse guidance for medium-range air-to-air missiles. *Journal of Guidance, Control and Dynamics*, *13*(4), 603–608.

Imado, F., & Kuroda, T., 1992. Optimal midcourse guidance systems against hypesonic targets. In *Proceedings of the AIAA Guidance and Control Conference* (pp. 1006–1011).

Keerthi, S. S., & Gilbert, E. G. (1988). Optimal infinite horizon feedback laws for a general class of constrained discrete time systems. *Journal of Optimisation Theory and its Applications*, *57*, 265–293.

Mayne, D. Q., & Michalska, H. (1990). Receding horizon control of nonlinear systems. *IEEE Transactions on Automatic Control*, *35*, 814–824.

Menon, P. K. A., & Briggs, M. M. (1990). Near-optimal midcourse guidance for air-to-air missiles. *Journal of Guidance, Control and Dynamics*, *13*(4), 596–602.

Michalska, H., & Mayne, D. Q. (1991). Receding horizon control of nonlinear systems without differentiablility of optimal value function. *Systems and Control Letters*, *16*, 123–130.

Rusnak, I. (1996). Analytical missile guidance laws with time-varying transformation. *Journal of Guidance, Control and Dynamics*, *19*(2), 496–499.

Song, E. J., & Tahk, M. T. (1998). Real-time midcourse guidance law with interception point prediction. *Control Engineering Practice*, *6*, 957–967.